Dybal, J. & Krimm, S. Normal-mode analysis of infrared and raman spectra of crystalline isotactic poly(methyl methacrylate). Macromolecules 23, 1301-1308

2 AUTHORS, INCLUDING:

Jiri Dybal
Academy of Sciences of the Czech Republic

188 PUBLICATIONS **2,810** CITATIONS

added 1.0 g (2.8 mmol) of Cl(n-Bu)$_2$SiSi(n-Bu)$_2$Cl in 5 mL of dry THF, and the solution was refluxed for 22 h. After the usual workup, 1.34 g of crude polymer was obtained as clear viscous liquid.

In an alternate synthesis, the dilithium reagent was prepared from 0.97 g (2.9 mmol) of HC≡CSi(n-Bu)$_2$Si(n-Bu)$_2$C≡CH and 3.65 mL (5.84 mmol) of 1.6 M n-BuLi hexane solution, in 20 mL of dry THF. To the dilithium reagent was added 0.52 g (2.8 mmol) of ClMe$_2$SiSiMe$_2$Cl in 5 mL of dry THF, and the solution was refluxed for 22 h. After the ususal workup, 1.12 g of crude polymer was obtained as a clear viscous ligand. UV: λ_{max} 214 (sh), 226, 240 (sh) nm (THF solution).

Note Added in Proof. A recent communication reports the synthesis of polymers similar to these by ring opening of the 8-membered ring dimer: Ishikawa, M.; Hasegawa, Y.; Hatana, T.; Kunai, A. *Organometallics* 1989, *8*, 2741. We have also observed ring-opening polymerization and will report it later.

References and Notes

(1) (a) Ishikawa, M. *Pure Appl. Chem.* 1978, *50*, 11. (b) Ishikawa, M.; Kumada, M. *Adv. Organomet. Chem.* 1981, *19*, 51. (c) Sakurai, H. *J. Organomet. Chem.* 1980, *200*, 261.
(2) Sakurai, H.; Kira, M.; Sugiyama, H., in press. Sakurai, H. In *Silicon Chemistry*; Corey, J. Y., Corey, E. R., Gaspar, P. P., Eds.; Ellis Horwood Ltd.; Chichester, U.K., 1987.
(3) For an alternate assignment involving 2pπ–3dπ charge transfer see: (a) Shizuka, H.; Obuchi, H.; Ishikawa, M.; Kumada, M. *J. Chem. Soc., Chem. Commun.* 1981, 405. (b) Shizuka, H.; Sato, Y.; Ishikawa, M.; Kumada, M. *Ibid.* 1982, 439. (c) Shizuka, H.; Sato, Y.; Ueki, Y.; Ishikawa, M.; Kumada, M. *J. Chem. Soc., Faraday Trans. 1* 1984, *80*, 341. (d) Shizuka, H.; Obuchi, H.; Ishikawa, M.; Kumada, M. *Ibid.* 1984, *80*, 383.
(4) Gilman, H.; Atwell, W. H., Schwebke, G. C. *J. Organomet. Chem.* 1946, *2*, 369.
(5) Sakurai, H.; Kumada, M. *Bull Chem. Soc. Jpn.* 1964, *37*, 1894.
(6) Sakurai, H.; Nakadaira, Y.; Hosomi, A.; Eriyama, Y.; Kabuto, C. *J. Am. Chem. Soc.* 1983, *105*, 3359.
(7) (a) Nate, K.; Ishikawa, M.; Ni, H.; Watanabe, H.; Saheki, Y. *Organometallics* 1987, *6*, 1673. (b) Shinya, K. *J. Organomet. Chem.* 1986, *310*, C57.
(8) The reaction of the di-Grignard reagents with 1,2-dichlorodisilanes in dilute (0.1 M) THF solution led to the formation of the eight-membered ring disilanyleneacetylene. See: Iwahara, T.; West, R. *J. Chem. Soc., Chem. Commun.* 1988, *14*, 954.
(9) Sakurai, H.; Tominaga, K.; Watanabe, T.; Kumada, M. *Tetrahedron Lett.* 1966, *45*, 5493.
(10) Seabald, A.; Seiberlich, P.; Wrackmeyer, B. *J. Organomet. Chem.* 1986, *303*, 73.
(11) Skattebol, L.; Jones, E. R. H.; Whiting, M. C. *Organic Syntheses*; Wiley: New York, 1963; Collect. Vol. 4, p 792.

Normal-Mode Analysis of Infrared and Raman Spectra of Crystalline Isotactic Poly(methyl methacrylate)

J. Dybal and S. Krimm[*,†]

Institute of Macromolecular Chemistry, Czechoslovak Academy of Sciences, 162 06 Prague 6, Czechoslovakia, and Biophysics Research Division and Department of Physics, University of Michigan, Ann Arbor, Michigan 48109. Received November 29, 1988; Revised Manuscript Received June 9, 1989

ABSTRACT: Infrared spectra of oriented and Raman spectra of nonoriented samples of crystalline isotactic poly(methyl methacrylate) (i-PMMA) have been measured. These vibrational spectra have been analyzed by means of normal-mode calculations, using a combined valence force field transferred without refinement from hydrocarbons and from methyl acetate. Calculations have been done for single chain 5/1 and 10/1 helical backbone conformations. Best agreement in the low-frequency region is found between the observed and calculated frequencies for the 10/1 structure. Infrared and Raman bands over the entire spectral region can be satisfactorily interpreted on the basis of the potential energy distributions and dispersion curves for the 10/1 helical conformation of the single i-PMMA chain in the double-stranded structure.

Introduction

Infrared and Raman spectroscopy, in combination with normal mode calculations, provide a powerful tool for structural analyses of polymers. We present here such a study of the structure and spectrum of isotactic poly(methyl methacrylate) (i-PMMA).

There have been several reports of infrared and Raman spectra and tentative band assignments for (i-PMMA).[1–11]

Differently deuterated i-PMMA samples were used in the analyses of the C–H stretch and bend modes.[2,6,7] Bands exhibiting temperature dependences in the infrared spectra of i-PMMA in bulk and in solution were assigned to various conformational forms.[3,8,9] Characteristic solid-state infrared bands of the crystalline and the amorphous phases were determined.[10,11] Using a Urey–Bradley force field refined for polyesters, normal-mode calculations of the low-frequency skeletal modes have been performed on 5/1 helical chain models of i-PMMA.[5] How-

† University of Michigan.

Table I
Local Symmetry Coordinates for Isotactic Poly(methyl methacrylate)

symmetry coordinate	descriptn[a]
Alkyl Part	
$S_1 = \Delta(r_{15} + r_{52})/(2)^{1/2}$	CC s1
$S_2 = \Delta(r_{15} - r_{52})/(2)^{1/2}$	CC s2
$S_3 = \Delta(r_{67} + r_{68} + r_{69})/(3)^{1/2}$	α-CH$_3$ ss
$S_4 = \Delta(2r_{67} - r_{68} - r_{69})/(6)^{1/2}$	α-CH$_3$ as2
$S_5 = \Delta(r_{68} - r_{69})/(2)^{1/2}$	α-CH$_3$ as1
$S_6 = \Delta r_{56}$	$C^\alpha C^\beta$ s
$S_7 = \Delta(r_{23} + r_{24})/(2)^{1/2}$	CH$_2$ ss
$S_8 = \Delta(r_{23} - r_{24})/(2)^{1/2}$	CH$_2$ as
$S_9 = \Delta(\theta_{156} + \theta_{152} + \theta_{256} - \theta_{1,5,10} - \theta_{6,5,10} - \theta_{2,5,10})/(6)^{1/2}$	CC$^\alpha$C d
$S_{10} = \Delta(2\theta_{152} - \theta_{156} - \theta_{256})/(6)^{1/2}$	C$^\beta$ b1
$S_{11} = \Delta(\theta_{156} - \theta_{256})/(2)^{1/2}$	C$^\beta$ b2
$S_{12} = \Delta(2\theta_{6,5,10} - \theta_{1,5,10} - \theta_{2,5,10})/(6)^{1/2}$	C* b1
$S_{13} = \Delta(\theta_{1,5,10} - \theta_{2,5,10})/(2)^{1/2}$	C* b2
$S_{14} = \Delta(\theta_{768} + \theta_{769} + \theta_{869} - \theta_{567} - \theta_{568} - \theta_{569})/(6)^{1/2}$	α-CH$_3$ sb
$S_{15} = \Delta(2\theta_{869} - \theta_{768} - \theta_{769})/(6)^{1/2}$	α-CH$_3$ ab1
$S_{16} = \Delta(\theta_{768} - \theta_{769})/(2)^{1/2}$	α-CH$_3$ ab2
$S_{17} = \Delta(2\theta_{567} - \theta_{568} - \theta_{569})/(6)^{1/2}$	α-CH$_3$ r1
$S_{18} = \Delta(\theta_{568} - \theta_{569})/(2)^{1/2}$	α-CH$_3$ r2
$S_{19} = \Delta(5\theta_{5,2,17} - \theta_{523} - \theta_{524} - \theta_{324} - \theta_{3,12,17} - \theta_{4,2,17})/(30)^{1/2}$	C$^\alpha$CC$^\alpha$ d
$S_{20} = \Delta(4\theta_{324} - \theta_{523} - \theta_{524} - \theta_{3,2,17} - \theta_{4,2,17})/(20)^{1/2}$	CH$_2$ b
$S_{21} = \Delta(\theta_{523} + \theta_{524} - \theta_{3,2,17} - \theta_{4,2,17})/2$	CH$_2$ w
$S_{22} = \Delta(\theta_{523} - \theta_{524} + \theta_{3,2,17} - \theta_{4,2,17})/2$	CH$_2$ r
$S_{23} = \Delta(\theta_{523} - \theta_{524} - \theta_{3,2,17} + \theta_{4,2,17})/2$	CH$_2$ t
$S_{24} = \Delta\tau_{5,6}$	C$^\alpha$C$^\beta$ tor
$S_{25} = \Delta\tau_{1,5}$	CC$^\alpha$ tor
$S_{26} = \Delta\tau_{5,2}$	C$^\alpha$C tor
Ester Part	
$S_{27} = \Delta r_{5,10}$	C$^\alpha$C* s
$S_{28} = \Delta r_{10,11}$	CO s
$S_{29} = \Delta r_{10,12}$	C–O s
$S_{30} = \Delta r_{12,13}$	O–C s
$S_{31} = \Delta(r_{13,14} + r_{13,15} + r_{13,16})/(3)^{1/2}$	OCH$_3$ ss
$S_{32} = \Delta(2r_{13,14} - r_{13,15} - r_{13,16})/(6)^{1/2}$	OCH$_3$ as2
$S_{33} = \Delta(r_{13,15} - r_{13,16})/(2)^{1/2}$	OCH$_3$ as1
$S_{34} = \Delta(2\theta_{5,10,12} - \theta_{5,10,11} - \theta_{11,10,12})/(6)^{1/2}$	CCO d
$S_{35} = \Delta(\theta_{5,10,11} - \theta_{11,10,12})/(2)^{1/2}$	CO ib
$S_{36} = \Delta\pi$	CO ob
$S_{37} = \Delta\theta_{10,12,13}$	COC d
$S_{38} = \Delta(\theta_{14,13,15} + \theta_{14,13,16} + \theta_{15,13,16} - \theta_{12,13,14} - \theta_{12,13,15} - \theta_{12,13,16})/(6)^{1/2}$	OCH$_3$ sb
$S_{39} = \Delta(2\theta_{15,13,16} - \theta_{14,13,15} - \theta_{14,13,16})/(6)^{1/2}$	OCH$_3$ ab1
$S_{40} = \Delta(\theta_{14,13,15} - \theta_{14,13,16})/(2)^{1/2}$	OCH$_3$ ab 2
$S_{41} = \Delta(2\theta_{12,13,14} - \theta_{12,13,15} - \theta_{12,13,16})/(6)^{1/2}$	OCH$_3$ r1
$S_{42} = \Delta(\theta_{12,13,15} - \theta_{12,13,16})/(2)^{1/2}$	OCH$_3$ r2
$S_{43} = \Delta\tau_{10,12}$	C*–O tor
$S_{44} = \Delta\tau_{12,13}$	O–C tor
$S_{45} = \Delta\tau_{5,10}$	C$^\alpha$C* tor

[a] Abbreviations: s, stretch; as, antisymmetric stretch; ss, symmetric stretch; b, bend; ab, antisymmetric bend; sb, symmetric bend; ib, in-plane bend; ob, out-of-plane bend; d, deformation; r, rock; w, wag; t, twist; tor, torsion.

Table II
Force Constants for Isotactic Poly(methyl methacrylate)

force const	value[c]
Alkyl Part:[a] C–CH$_3$ Group	
f(CH)	4.699
f(HCH)	0.540
f(CCH)	0.645
f(CH′,CH″)	0.043
f(CCH′,CCH″)	−0.012
f(C$^\alpha$–C$^\beta$ torsion)	0.072
Alkyl Part:[a] C–CH$_2$–C Group	
f(CH)	4.554
f(HCH)	0.550
f(CCH)	0.656
f(CCC)	1.130
f(CH′,CH″)	0.006
f(CCH′,CCH″)	−0.021
f(HCC′,CC″)	0.079
f(HCC′,HCC″)	0.012
f(HCC,CCC′)	−0.031
Alkyl Part:[a] Rest of Force Constants	
f(CC)	4.337
f(CCC)	1.086
f(C–C torsion)	0.024
f(CC′,CC″)	0.101
f(CC,CCH)	0.328
f(CC,CCC′)	0.417
f(CCC′,CCC″)	−0.041
f(HCC,CCC′-trans)	0.049
f(HCC,CCC′-gauche)	−0.052
f(C′CC,CCC″-trans)	−0.011
f(C′CC,CCC″-gauche)	0.011
Ester Part[b]	
f(27,27)	4.046
f(28,28)	11.009
f(29,29)	5.031
f(30,30)	5.062
f(31,31)	5.050
f(32,32)	4.859
f(33,33)	4.789
f(34,34)	1.129
f(35,35)	1.259
f(36,36)	0.734
f(37,37)	1.729
f(38,38)	0.661
f(39,39)	0.485
f(40,40)	0.518
f(41,41)	0.868
f(42,42)	0.835
f(43,43)	0.210
f(44,44)	0.032
f(45,45)	0.024
f(28,29)	0.971
f(27,28)	0.971
f(30,32)	−0.639
f(29,30)	0.731
f(29,35)	−0.219
f(27,35)	0.219

[a] Force constants in terms of internal coordinates. [b] Force constants in terms of local symmetry coordinates of Table I. [c] Units are mdyn/Å for stretch and stretch, stretch force constants, mdyn for stretch, bend force constants, and mdyn Å for all others.

ever, there has as yet been no definitive, full interpretation of the vibrational spectra of i-PMMA.

In this paper we present further experimental studies and the results of normal-mode calculations of i-PMMA. We have measured the infrared and Raman spectra of partially crystalline i-PMMA, prepared by annealing solid samples.[5,12,13] Polarized infrared spectra of oriented and Raman spectra of nonoriented crystalline i-PMMA samples have been obtained. In the normal-mode calculations, we used valence force constants refined for branched hydrocarbons[14] and for methyl acetate.[15]

The structure of i-PMMA has been the subject of controversy. Stroupe and Hughes[16] proposed a 5/2 helix, but subsequent X-ray[17] and X-ray plus far infrared and

normal mode[5] studies suggested a 5/1 helical backbone conformation. After an intramolecular energy calculation indicated that a 12/1 helix chain was more stable than a 5/1 helix,[18] the X-ray pattern was reexamined and found to be more consistent with a double helix of 10/1 chains.[19] This was subsequently disputed on the basis of X-ray studies of crystalline[20] and noncrystalline[21] i-PMMA. However, the 10/1 helix structure has been supported by virtual bond[22] and conformational energy[23,24] calculations and by a combined X-ray diffraction and energy calculation study.[25]

Table III
Observed and Calculated Frequencies (cm^{-1}) of Selected Vibrations of Isotactic Poly(methyl methacrylate)

obsd			calcd				potential energy
infrared[a]			10/1 helix		5/1 helix		distributn[b] 5/1 helix
‖	⊥	Raman	A	E_1	A	E_1	
1268			1252		1266		CH_2 t(41), CC s1(14)
1198			1202		1212		C–O s(20), CH_2 w(12)
1154		1150	1147		1170		CH_2 t(23), α-CH_3 r1(16), CC s1(13)
	1115			1127		1090	α-CH_3 r1(22), CH_2 t(19), $C^{\alpha}C^{\beta}$ s(16)
	932			954		940	CH_2 r(26), α-CH_3 r1(22), CC s2(13)
	846			854		864	CH_2 r(17), $C^{\alpha}C$ s(15), $C^{\alpha}C^*$ s(13)
	609⎫ 559⎭			603		637	$C^{\alpha}C^*$ s(21), CO ib(17), $CC^{\alpha}C$ d(13)
559		597⎫ 562⎭	602		627		$C^{\alpha}C^*$ s(26), CO ib(20), $CC^{\alpha}C$ d(13)
	480	481		466		484	CCO d(16), CC s1(14)
476			467		464		CCO d(21), C* b1(17)
	406	390		380		443	C^{β} b2(21), $CC^{\alpha}C$ d(13)
365		372	366		391		C^{β} b2(30), $CC^{\alpha}C$ d(11)
	368			345		355	COC d(23), C^{β} b2(13), C* b1(21)
		341	335		338		COC d(33), CO ib(25), C* b1(21)
	338			325		339	CO ib(25), COC d(23), C* b1(20)
314		314	309		295		$CC^{\alpha}C$ d(31), C* b2(11)
	232			252		273	$CC^{\alpha}C$ d(25), C^{β} b2(20)
		221	235		261		C* b2(27), C–O tor(21), C^{β} b2(21)
217			206		201		C* b1(20), $C^{\alpha}C^*$ tor(19), C^{β} b2(17)

[a] Infrared bands: ‖, parallel dichroism; ⊥, perpendicular dichroism. [b] Abbreviations: s, stretch; b, bend; ib, in-plane bend; d, deformation; r, rock; w, wag; t, twist; tor, torsion. Only contributions 10% or greater are included.

Distinctions between different local conformations of a regular polymer chain can be made on the basis of normal-mode analyses of the vibrational spectrum, since the infrared and Raman bands, particularly in the low-frequency region, are sensitive to the three-dimensional arrangement of the atoms. This has been amply demonstrated on macromolecules as diverse as polyethylene,[26] poly(vinyl chloride),[27] and polypeptides.[28] We have used the same approach here, calculating the normal modes of the 5/1 and 10/1 helical structures of i-PMMA and comparing these predictions with the observed bands for the crystalline polymer. Since the force fields used in the calculations[14,15] have proven to be highly successful in accounting for observed spectra of related molecules, we can expect the predictions for i-PMMA to result in meaningful distinctions in structure. This is the case, with the 10/1 helical conformation being clearly favored. We discuss this determination first and then present a more detailed analysis of the spectrum of the 10/1 helix structure.

Experimental Section

The sample of isotactic PMMA used in the present study was kindly supplied by Dr. R. O. Loutfy from Xerox Research Center of Canada. The tacticity of the polymer sample was determined on the basis of proton NMR spectra: the content of isotactic triads is higher than 98%.[29]

Films of i-PMMA were prepared by casting of toluene solutions on an aluminum foil and subsequent room-temperature evaporation of the solvent. Samples for Raman measurements consisted of about fifty layers of such films. For infrared measurements, oriented samples were obtained by stretching the films (in water at 50 °C) 10–15 times their original length. Crystallinity was induced by then annealing in a vacuum oven at 120 °C for 8 days. This temperature is optimum with respect to the crystallization rate.[12,13] Polarized infrared spectra were obtained with the electric vector parallel and perpendicular to the stretching direction. No polarization results are available for the Raman spectra because the sample used in the measurements had no defined orientation.

Raman spectra were obtained with a Spex 1403 double monochromator equipped with holographic gratings. Spectra were excited by the 514.5-nm line of a Coherent Radiation 52 argon ion laser, and 90° scattering geometry was used. Infrared spectra were recorded on a Bomem DA3 FTIR spectrometer.

Normal-Mode Calculations

The normal-mode calculations were done on regular single chain 5/1[5] and 10/1[19] helical structures. This is a reasonable approximation, since the interchain forces are weak in comparison to the intrachain; though they may determine the chain conformation, they do not influence its frequencies significantly (possibly giving rise to small band shifts and/or splittings). The specific three-dimensional structure that results from these interactions is primarily responsible for its characteristic frequency distribution.

The following structural parameters (bond lengths and bond angles) were used in the normal-mode calculations: $CC^{\alpha} = C^{\alpha}C = C^{\alpha}C^{\beta} = 1.53$ Å, $C^{\alpha}C^* = 1.51$ Å, CH = 1.09 Å, $C^*O^* = 1.21$ Å, $C^*O = 1.34$ Å, OC = 1.46 Å, $C^{\alpha}C^*O^* = 127°$, $C^{\alpha}C^*O = 122°$, $C^*OC = 117°$. The ester group was assumed to be in a planar conformation. The bond lengths and bond angles of the ester group were taken from the results of the ab initio optimization of the methyl acetate molecular geometry.[30] The bond angles in both the ester and α-methyl groups were assumed to be tetrahedral. According to the results of the X-ray studies[5,19] and the conformational energy calculations,[23,24] both bond angles in the chain backbone are appreciably distorted relative to the tetrahedral value. In the present calculations, however, the main-chain angles were kept tetrahedral in order to ensure transferability of the force constants. Cartesian coordinates were calculated for the ideal 5/1 and 10/1 helical structures of the isolated i-PMMA chain, with alternating skeletal torsion angles of 0° and 72° and of 0° and 36°, respectively. All the ester groups were assumed to be parallel, with the OCH_3 group oriented trans with respect to the α-CH_3 group. The symmetry coordinates, constructed from the internal coordinates defined in the standard way, are listed in Table I with the numbering of atoms shown in Figure 1.

The optically active modes of an infinite, isolated i-PMMA chain with helical conformation are classified into

Table IV
Observed and Calculated Frequencies (cm⁻¹) of Isotactic Poly(methyl methacrylate)

obsd			calcd			
infrared[a]		Raman	A	E₁	E₂	potential energy distributn[b]
‖	⊥					
3029		3027	3025	3025	3025	OCH_3 as2(99)
3005	3005	3006	3002	3002	3002	OCH_3 as1(99)
			2961			α-CH_3 as2(96)
				2961		α-CH_3 as2(80), α-CH_3 as1(20)
					2961	α-CH_3 as1(54), α-CH_3 as2(45)
2955	2954	2953	2961			α-CH_3 as1(96)
				2961		α-CH_3 as1(80), α-CH_3 as2(20)
					2961	α-CH_3 as2(54), α-CH_3 as1(45)
			2961	2961	2961	OCH_3 ss(100)
2912	2914	2919	2928	2928	2928	CH_2 as(99)
2880	2880		2882	2882	2882	α-CH_3 ss(100)
2841	2840	2842	2856	2856	2856	CH_2 ss(99)
1733	1736	1738,1725	1749	1749	1749	CO s(82), CCO d(10)
1486		1486	1473			CH_2 b(54), α-CH_3 ab1(34)
	1486			1472		CH_2 b(47), α-CH_3 ab1(40)
					1470	α-CH_3 ab1(54), CH_2 b(33)
			1467			α-CH_3 ab2(90)
				1467		α-CH_3 ab2(89)
					1467	α-CH_3 ab2(85)
			1462			α-CH_3 ab1(55), CH_2 b(39)
				1462		α-CH_3 ab1(48), CH_2 b(45)
					1461	CH_2 b(63), α-CH_3 ab1(30)
1454	1453		1456	1456	1456	OCH_3 ab2(84), OCH_3 r2(16)
1442	1442	1447	1445	1445	1445	OCH_3 sb(95)
1432	1433	1432	1426	1426	1426	OCH_3 ab1(72), OCH_3 r1(24)
					1392	α-CH_3 sb(69)
	1386			1390		α-CH_3 sb(76)
1386		1388	1389			α-CH_3 sb(78)
					1337	α-CH_3 sb(25), CH_2 w(21), $C^\alpha C^*$ s(17), CH_2 t(13)
	1338	1335		1329		CH_2 w(34), CC s2(19), α-CH_3 sb(16), $C^\alpha C^*$ s(15)
1329			1325			CH_2 w(39), CC s2(25), $C^\alpha C^*$ s(14), α-CH_3 sb(14)
					1325	CH_2 w(47), CC s2(32)
	1298			1315		CC s2(32), CH_2 w(29), $C^\alpha C^*$ s(14)
1296			1310			CC s2(31), CH_2 w(23), $C^\alpha C^*$ s(15), C–O s(12)
					1267	CC s1(22), $C^\alpha C^\beta$ s(12), CC s2(12)
	1252			1259		CC s1(24), CH_2 t(15), $C^\alpha C^\beta$ s(13), $C^\alpha CC^\alpha$ d(10)
1268		1270	1252			CC s1(28), CH_2 t(22), $C^\alpha C^\beta$ s(14), $C^\alpha CC^\alpha$ d(12)
		1231			1231	C–O s(27), CH_2 t(26), CO ib(11)
	1198			1208		CH_2 t(21), C–O s(18), OCH_3 r1(14)
1198			1202			OCH_3 r1(24), C–O s(16), OCH_3 ab1(11)
1190		1190	1192			CH_2 t(26), CH_2 w(19), OCH_3 r1(13)
	1190			1188		OCH_3 r1(33), CH_2 t(20), OCH_3 ab1(11)
					1187	OCH_3 r1(47), OCH_3 ab1(16), COC d(11)
			1178			CH_2 t(36), OCH_3 r1(17)
	1150			1177		CH_2 w(17), CH_2 t(14), α-CH_3 r1(12)
		1157			1156	CH_2 w(19), α-CH_3 r2(16), CC s2(11), CH_2 t(11)
1154		1150	1147			$C^\alpha C^\beta$ s(14), CH_2 w(13), CH_2 t(13), O–C s(10)
		1123		1129		OCH_3 r2(51), OCH_3 ab2(10)
					1128	OCH_3 r2(82), OCH_3 ab2(16)
1115		1113	1128			OCH_3 r2(82), OCH_3 ab2(16)
	1115			1127		OCH_3 r2(32), CH_2 t(12)
					1100	CH_2 t(22), CH_3 r1(17), $C^\alpha C^\beta$ s(16), O–C s(11)
998		996	1036			O–C s(77), OCH_3 r1(10)
	998			1036		O–C s(76), OCH_3 r1(10)
					1034	O–C s(71), OCH_3 r1(10)
951			969			α-CH_3 r1(54), CH_2 r(21)
		960			968	α-CH_3 r2(34), α-CH_3 r1(23), CC s2(15), CH_2 r(12)
	953	953		966		α-CH_3 r1(48), CH_2 r(21)
	932	931		954		α-CH_3 r2(51), CC s2(30)
937			952			α-CH_3 r2(59), CC s2(32)
					946	CC s2(20), α-CH_3 r1(20), α-CH_3 r2(18), CH_2 r(16)
					860	$C^\alpha C^\beta$ s(22), CH_2 r(15), $C^\alpha C^*$ s(14), C–O s(13)
	846			854		$C^\alpha C^\beta$ s(24), CH_2 r(17), C–O s(14), $C^\alpha C^*$ s(13)
843		844	853			$C^\alpha C^\beta$ s(26), CH_2 r(18), C–O s(14), $C^\alpha C^*$ s(12)
810		809	804			$C^\alpha C^\beta$ s(24), C–O s(10)
	808			803		$C^\alpha C^\beta$ s(23), C–O s(10)
					800	$C^\alpha C^\beta$ s(19), C–O s(10)
		782			778	CO ob(52), C* b2(11)
	764			772		CO ob(61), C* b2(12)
758		764	770			CO ob(64), C* b2(12)
					606	$C^\alpha C^*$ s(26), CO ib(18), $CC^\alpha C$ d(10)
	609} 559}			603		$C^\alpha C^*$ s(30), CO ib(21)

Table IV (Continued)

obsd			calcd			
infrared[a]						
∥	⊥	Raman	A	E₁	E₂	potential energy distributn[b]
559		59? / 562	602			C^αC* s(31), CO ib(22)
					481	CC sl(22), CCO d(11)
	480	481		466		CCO d(22), CC^αC d(19), C* b1(16)
476			467			CC^αC d(22), CCO d(21), C* b1(17), CH₂ r(12)
		464			455	CC^αC d(17), CCO d(12), C^β b2(10)
	406	390		380		C^β b2(27), C* b2(12), CC^αC d(10)
365		372	366			COC d(25), CC^αC d(16), C* b2(15)
					359	COC d(24), CC^αC d(16), C^β b2(13)
	368			345		COC d(36), CO ib(15), C* b1(10)
					337	CO ib(25), COC d(22), C* b1(19)
		341	335			CO ib(21), C* b1(21), COC d(20)
	338			325		CC^αC d(30), C* b1(15), CO ib(12)
314		314	309			C^β b2(32), CC^αC d(21)
					268	C^β b2(32), CC^αC d(17), C* b1(14), C^β b1(10)
	232			252		C^β b2(39), C* b2(13), C-O tor(11)
		221	235			C-O tor(34), C^β b2(25), C* b2(24)
217			206			CCO d(36), C* b1(35), COC d(11)
			202			C^αC^β tor(30), CCO d(21), C* b1(19), C-O tor(12)
					201	C^αC^β tor(33), CCO d(17), C-O tor(11)
					197	C^αC^β tor(50), C-O tor(18)
		195				C^αC^β tor(97)
	188			193		C^αC^β tor(70), CCO d(10)
					185	C-O tor(29), CCO d(16), C^αC^β tor(16), C* b1(14)
				164		C-O tor(25), O-C tor(21)
165			144			O-C tor(65), C* b2(17)
					133	O-C tor(62)
	140			128		O-C tor(68), C-O tor(17)
					115	C^β b1(20), O-C tor(19), C-O tor(16), C^αCC^α d(15)
109			110			C-O tor(41), O-C tor(29), C^α b2(18)
	113			86		C* b2(29), C^β b1(16), C^αC* tor(15)
		85	72			CC sl(36), C^β b1(27), C^αCC^α d(11)
					71	C^αCC^α d(28), C* b2(24), C^αC* tor(15)
				47		C^αCC^α d(39), C^αC* tor(23), C^β b1(22)
			44			C^αC* tor(88)
					39	C^αC* tor(75)
				36		C^αC* tor(58), C^αCC^α d(12)
			24			C^αCC^α d(55), C^β b1(35)
					17	C^αC tor(58), CC^α tor(27)
				8		C^αC tor(45), CC^α tor(38)
					7	CC^α tor(53), C^αC tor(24)

[a] Infrared bands: ∥, parallel dichroism; ⊥, perpendicular dichroism. [b] Abbreviations: s, stretch; as, antisymmetric stretch; ss, symmetric stretch; b, bend; ab, antisymmetric bend; sb, symmetric bend; ib, in-plane bend; ob, out-of-plane bend; d, deformation; r, rock; w, wag; t, twist; tor, torsion. Only contributions 10% or greater are included.

A, E₁, and E₂ symmetry species, where the phase differences between the motions in adjacent monomer units are 0°, 72°, and 144° for the 5/1 helix and 0°, 36°, and 72° for the 10/1 helix, respectively. The former two species are both infrared and Raman active, and the last is Raman active only. In the infrared dichroic spectrum, the A modes are polarized parallel and the E₁ modes perpendicular to the helix axis.

The force constants for the aliphatic chain were taken to be those determined by Snyder and Schachtschneider for branched hydrocarbons.[14] The force constants for the ester group were taken directly from our work on methyl acetate.[15] Using this combined force field, we obtained good agreement between the observed frequencies of i-PMMA and those calculated for the 10/1 helical structure. A tentative refinement of specific force constants by a least-squares iteration did not significantly improve the overall fit between the observed and calculated frequencies. Therefore, rather than undertake a refinement based on the assumed geometry, the combined valence force fields transferred from hydrocarbons and methyl acetate (listed in Table II) were used without modification in the normal-mode analysis of i-PMMA. This permits one to have greater confidence in the results of the calculations, which provide practically complete assignments for the observed vibrational spectra, even though the frequency agreement in some cases is poor.

Results and Discussion

Raman spectra of the annealed i-PMMA sample (partially crystalline) and of the sample prepared by solvent evaporation without annealing (amorphous) are shown in Figure 2. Several differences can be observed between the spectra of crystalline and amorphous i-PMMA, which are characteristic of a transition from unordered to ordered polymer. The bands in the spectrum of crystalline i-PMMA are much sharper and many of them exhibit frequency shifts and changes in intensity, e.g., the peaks in regions 1200–1000 cm⁻¹ and 1000–900 cm⁻¹. In the spectrum of the crystalline form, a new band at 314 cm⁻¹ is observed that does not appear in the spectrum of the amorphous form. The mode near 372 cm⁻¹ is observed to split into two components in the spectrum of the crystalline sample, at 372 and 390 cm⁻¹. The band at 1729 cm⁻¹, corresponding to the C=O stretch vibration, is also split in the spectrum of the crystalline form, into a doublet at 1738 and 1725 cm⁻¹ (clearly visible in expanded
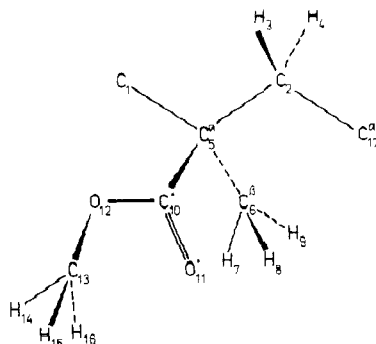
Figure 1. Structural unit of i-PMMA, with atom numbering.

Figure 2. Raman spectra of i-PMMA: (a) amorphous sample; (b) partially crystalline sample.

Figure 3. Polarized infrared spectra of oriented sample of partially crystalline i-PMMA, measured with the electric vector (a) perpendicular and (b) parallel to the draw direction.

spectra). Analogous splittings of the C=O stretch mode have been observed previously in the spectra of the ordered structures of syndiotactic PMMA.[31]

Differences in the infrared spectra between amorphous and partially crystalline samples have been discussed previously.[10,11] Bands characteristic of the amorphous phase were found at 1047 and 938 cm^{-1}, while characteristic bands of the crystalline phase were found at 1338, 1298, and 882 cm^{-1}. Polarized infrared spectra of the annealed oriented (partially crystalline) i-pMMA film are shown in Figure 3.

Some observed infrared and Raman frequencies are listed in Table III and compared with calculated frequencies of the 5/1 and 10/1 helical structures. In this table we list only the A and E$_1$ species modes above 600 cm^{-1} for which the calculated frequencies differ by 10 cm^{-1} or more and all the modes in the 600–200 cm^{-1} region. Experience has shown[5,32] that the low-frequency region is most sensitive to small changes in conformation of the chain backbone. (The E$_2$ species modes are not listed here since the assignments of low-frequency Raman bands to this species are less certain.)

As can be seen from Table III, the calculated frequencies of the 10/1 helix are in better agreement with the observed bands than are those of the 5/1 helix. The average difference between observed and calculated frequencies is 21.1 cm^{-1} for the 5/1 helix compared to 12.8 cm^{-1} for the 10/1 helix (the average difference for this helix over the spectral range of 1800–85 cm^{-1} is 11.6 cm^{-1}). Although there are some large discrepancies in the latter case, these results clearly show that the 10/1 helix is in better agreement with the observed infrared and Raman data than is the 5/1 helix. They thus provide additional support for this model of the chain conformation in the crystal structure of i-PMMA.

We turn now to a detailed analysis of the spectra of crystalline i-PMMA based on the 10/1 helix model of the chain conformation. The observed infrared and Raman band frequencies are listed in Table IV together with the calculated A, E$_1$, and E$_2$ normal-mode frequencies and potential energy distributions (PED). The experimental infrared frequencies in the region below 600 cm^{-1} are taken from the paper of Tadokoro et al.[5] Band assignments have been made on the basis of extensive spectral studies of isotopic derivatives of i-PMMA[2,6,7] as well as our infrared dichroism results. Since it is often difficult to assign Raman bands to specific species, we have in such cases associated the band with the A species mode. Dispersion curves are given in Figure 4.

The bands in the C–H stretch region, from 3100 to 2800 cm^{-1}, are probably affected by Fermi resonance between the C–H stretch fundamentals and overtones and combinations of lower frequency modes, which complicate the band assignments.[2,6,7,33] However, as can be
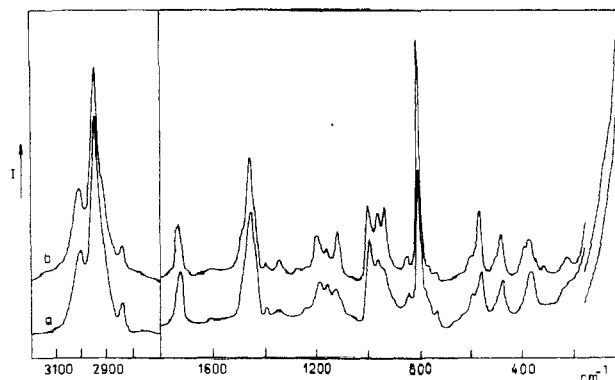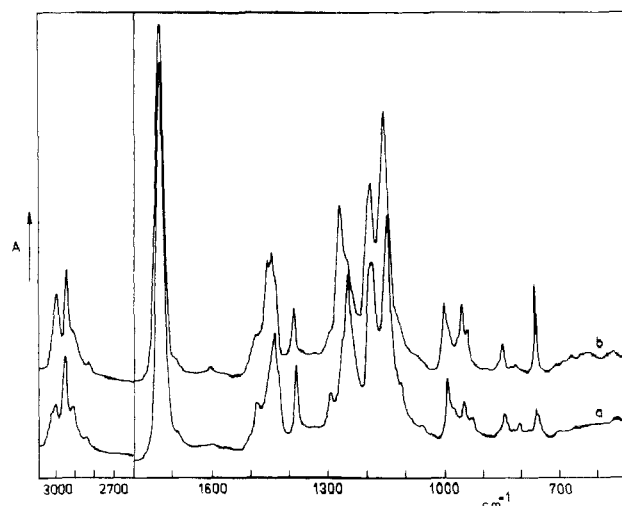
seen from Table IV, the results of the normal-mode calculations suggest a reasonable interpretation of the observed bands in this region that is in qualitative agreement with the conclusions of studies of specifically deuterated derivatives of i-PMMA.[6,7]

The splitting of the C=O stretch mode near 1730 cm^{-1}, observed in the spectra of crystalline i-PMMA, is not reproduced in our normal mode calculation of the isolated i-PMMA chain (Table IV). We believe that this splitting can be explained by resonance transition dipole interactions, which were not included in the calculations. This is similar to the observed splittings of the amide I and amide II modes in polypeptides[34-36] and the C=O stretch splitting in acid dimers,[34,37] both of which are satisfactorily reproduced when such interactions are included in the calculations.

The region from 1500 to 1350 cm^{-1} contains six bend modes of the methyl groups and one bend mode of the methylene group. The calculated frequencies in this region fit the observed data satisfactorily. The PEDs show that the α-CH$_3$ asymmetric bend 1 mixes with the CH$_2$ bend mode; all other methyl bends are well localized. The dispersion curves are essentially flat in this region. The bands in the region from 1350 to 1300 correspond to the CH$_2$ wag mode with considerable contributions from the backbone and side-chain CC stretch vibrations. The infrared bands in this region exhibit crystallization-sensitive behavior.[11]

The region from 1300 to 1050 cm^{-1} consists of mixed modes that are highly coupled along the chain, as indicated by the dispersion curves. This may account for
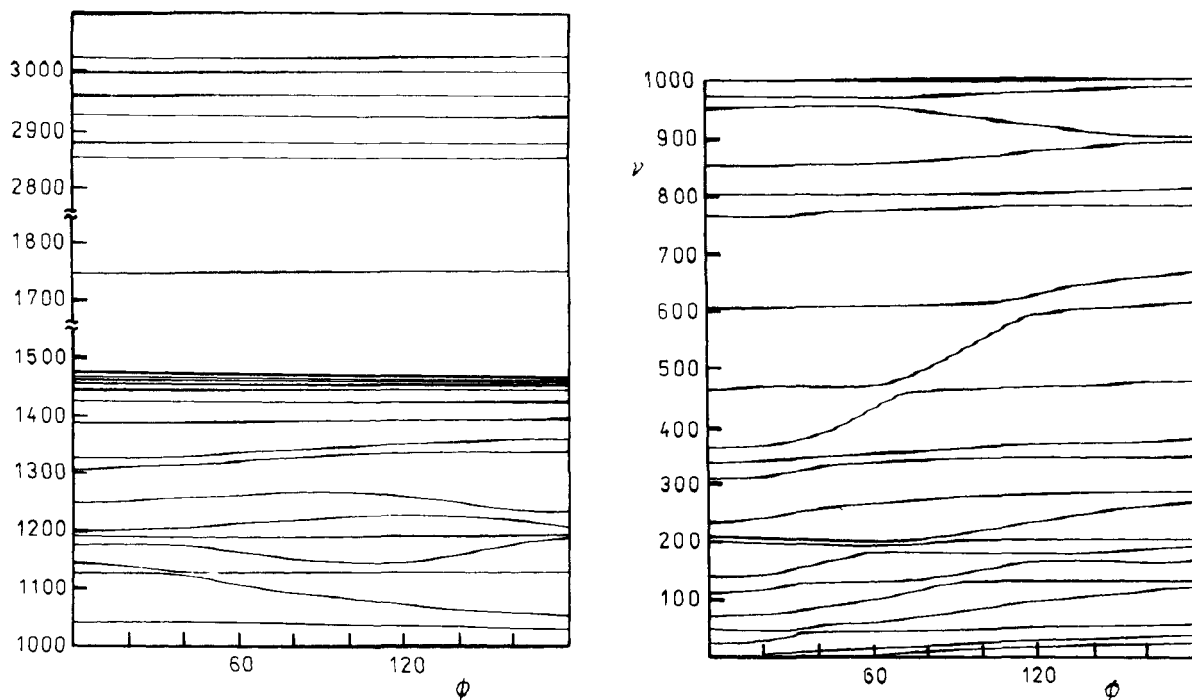
Figure 4. Dispersion curves for the single 10/1 i-PMMA chain.

some large discrepancies between observed and calculated frequencies, which would be sensitive to small changes in (presently unrefined) interaction force constants. The distinctive E_2 species C–O stretch + CH_2 twist mode at 1231 cm^{-1} is well predicted, as are the mixed modes with OCH_3 rock in the 1210–1190 cm^{-1} region. The observed band pattern in the 1160–1100 cm^{-1} region is reasonably well reproduced, except for the E_1 species mode calculated at 1177 cm^{-1}. As can be seen, the OCH_3 rock mode calculated at 1129 cm^{-1} completely changes its character in the A species vibration at 1147 cm^{-1}.

The bands near 998 cm^{-1} in the infrared and Raman spectra have been assigned to the OCH_3 rock vibration interacting with the stretch vibrations of the COC group.[2,6] Though this assignment is essentially confirmed by the normal coordinate calculations, the PED indicates large contributions from the O–C stretch vibration. As can be seen from Table IV, the observed frequencies of these modes are not well reproduced. Calculations show that the fit can be improved considerably by refinement of the f(C–O,O–C) force constant, without any practical change in the character of the vibration. However, since we decided to adhere strictly to transferability of force fields, we did not undertake this refinement. (In any case, it should properly be done only with the incorporation of the correct nontetrahedral geometry.) The observed weak band in the infrared spectrum with A component at 1058 cm^{-1} and E_1 component at 1064 cm^{-1} is not predicted by the normal-mode calculations. Since it appears also in the infrared spectrum of amorphous i-PMMA (at 1061 cm^{-1}), it is not a crystallinity-sensitive band. We suppose that this band belongs to a combination, probably 602 (A) + 467 (A) = 1069 (A) and 603 (E_1) + 467 (A) = 1070 (E_1).

Two α-CH_3 rock modes appear between 960 and 930 cm^{-1}, in agreement with the previous assignments.[2,6] (The weak perpendicular band at 980 cm^{-1} may be a combination: 602 (A) + 380 (E_1) = 982 (E_1).) The α-CH_3 rock mode at the lower frequency is coupled with the mixed vibration having A component near 850 cm^{-1}. This is illustrated by the corresponding dispersion curves, which

closely approach each other at high-phase angles. The characteristic band of the crystalline phase of i-PMMA found at 882 cm^{-1} in the infrared spectrum[11] is not predicted as a fundamental by the present normal-mode calculations. Its parallel character may be due to a combination band: 770 (A) + 110 (A) = 880 (A).

On the basis of the infrared and Raman spectra of i-PMMA, the bands observed near 760 cm^{-1} were assigned to the CH_2 rock mode[2] or to skeletal vibrations,[4] probably affected by the CH_2 rock vibration.[6] However, the calculated PED indicates that these modes contain predominantly C=O out-of-plane bend with contributions of side-chain bend motions. In the Raman spectra, a doublet occurs at 597 and 562 cm^{-1} and this doublet remains essentially unchanged during the transition of the i-PMMA sample from the unordered to the ordered state (Figure 2). According to the normal coordinate calculations, only one mode, $C^\alpha C^*$ stretch combined with C=O in-plane bend, is predicted in this frequency region. It is possible that the doublet is due to a Fermi resonance between the fundamental and a combination mode with components in the Raman: 372 (A) + 221 (A) = 593 (A). This is reasonable, since the fundamentals all involve motions essentially localized in the C–CO–O group (cf. PEDs in Table IV). It is interesting to note that a similar explanation can account for the doublet in the perpendicularly polarized infrared spectrum at 609 and 559 cm^{-1}: 372 (A) + 232 (E_1) = 604 (E_1). If, as observed in Figure 3, the two bands are of about the same intensity, the unperturbed fundamental would be at 584 cm^{-1}, diminishing the discrepancy with the calculated band.

As can be seen from Table IV, the low-frequency part of the vibrational spectrum contains several highly mixed modes. These modes are mainly due to the backbone and the ester group bend and, in the region below 230 cm^{-1}, significant contributions from six torsions. The dispersion curves indicate a great deal of coupling between the modes in the whole region below 700 cm^{-1}. While the frequency agreement in this region is not particularly good, the pattern of assignments is quite reasonable.

Conclusions

A comparison of observed low-frequency infrared and Raman bands with frequencies calculated for the 5/1 and 10/1 helix chain conformations of i-PMMA clearly favors the latter structure. The calculations on the 10/1 structure reproduce the overall frequencies fairly well, the average discrepancy between observed and calculated frequencies being 11.6 cm^{-1}. This is despite the assumption of a standard geometry for the backbone and the transfer without refinement of main-chain and side-chain force constants from hydrocarbons and methyl acetate. The calculated PEDs and dispersion curves provide insight into the vibrational behavior of the i-PMMA chains.

These calculations have been performed on a simple model structure of crystalline i-PMMA, i.e., the regular single 10/1 helix with parallel ester groups in a trans orientation. Energy calculations[23,24] indicate that interactions can lead, for example, to the stabilization of the antiparallel arrangement of the successive ester groups. Before such details of the conformational structure of i-PMMA can be analyzed by normal-mode calculations, further refinement of the force field, using isotopic derivatives and the observed chain geometry, is necessary. The present analysis provides a persuasive starting point for such a study.

References and Notes

(1) Baumann, U.; Schreiber, H.; Tessmar, K. *Makromol. Chem.* **1960**, *36*, 81.
(2) Nagai, H. *J. Appl. Polym. Sci.* **1963**, *7*, 1697.
(3) Havriliak, S.; Roman, N. *Polymer* **1966**, *7*, 387.
(4) Willis, H. A.; Zichy, V. J. I.; Hendra, P. *Polymer* **1969**, *10*, 737.[1]
(5) Tadokoro, H.; Chatani, Y.; Kusanagi, H.; Yokoyama, M. *Macromolecules* **1970**, *3*, 441.
(6) Schneider, B.; Štokr, J.; Schmidt, P.; Mihajlov, P.; Dirlikov, S.; Peeva, N. *Polymer* **1979**, *20*, 705.
(7) Dirlikov, S. K.; Koenig, J. L. *Appl. Spectrosc.* **1979**, *33*, 555.
(8) O'Reilly, J. M.; Mosher, R. A. *Macromolecules* **1981**, *14*, 602.
(9) Dybal, J.; Štokr, J.; Schneider, B. *Polymer* **1983**, *24*, 971.
(10) Spěváček, J.; Schneider, B.; Dybal, J.; Štokr, J. *Croat. Chem. Acta* **1987**, *60*, 11.
(11) Schneider, B.; Štokr, J.; Spěváček, J.; Baldrian, J. *Makromol. Chem.* **1987**, *188*, 2705.
(12) de Boer, A.; van Ekenstein, A.; Challa, G. *Polymer* **1975**, *16*, 930.
(13) Könnecke, K.; Rehage, G. *Colloid Polym. Sci.* **1981**, *259*, 1062.
(14) Snyder, R. G.; Schachtschneider, J. H. *Spectrochim. Acta* **1965**, *21*, 169.
(15) Dybal, J.; Krimm, S. *J. Mol. Struct.* **1988**, *189*, 383.
(16) Stroupe, J. D.; Hughes, R. E. *J. Am. Chem. Soc.* **1958**, *80*, 2341.
(17) Coiro, V. M.; DeSantis, P.; Liquori, A. M.; Mazzarella, L. *J. Polym. Sci., Part C* **1969**, *16*, 4591.
(18) Tadokoro, H.; Tai, K.; Yokoyama, M.; Kobayashi, M. *J. Polym. Sci., Polym. Phys. Ed.* **1973**, *11*, 825.
(19) Kusanagi, H.; Tadokoro, H.; Chatani, Y. *Macromolecules* **1976**, *9*, 531.
(20) Coiro, V. M.; Liquori, A. M.; De Santis, P.; Mazzarella, L. *J. Polym. Sci., Polym. Lett. Ed.* **1978**, *16*, 33.
(21) Lovell, R.; Windle, A. H. *Macromolecules* **1981**, *14*, 211.
(22) Sundararajan, P. R. *Macromolecules* **1979**, *12*, 575.
(23) Vacatello, M.; Flory, P. J. *Polym. Commun.* **1984**, *25*, 258.
(24) Vacatello, M.; Flory, P. J. *Macromolecules* **1986**, *19*, 405.
(25) Bosscher, F.; ten Brinke, G.; Eshius, A.; Challa, G. *Macromolecules* **1982**, *15*, 1364.
(26) Snyder, R. G. *J. Chem. Phys.* **1967**, *47*, 1316.
(27) Moore, W. H.; Krimm, S. *J. Mol. Spectrosc.* **1974**, *51*, 1.
(28) Krimm, S.; Bandekar, J. *Adv. Protein Chem.* **1986**, *38*, 181.
(29) Loutfy, R. O.; Teegarden, D. M. *Macromolecules* **1983**, *16*, 452.
(30) Van Alsenoy, C.; Scarsdale, J. N.; Schäfer, L. *J. Mol. Struct.* **1982**, *90*, 297.
(31) Dybal, J.; Spěváček, J.; Schneider, B. *J. Polym. Sci., Polym. Phys. Ed.* **1986**, *24*, 657.
(32) Dwivedi, A. M.; Krimm, S.; Malcolm, B. R. *Biopolymers* **1984**, *23*, 2025.
(33) Snyder, R. B.; Hsu, S. L.; Krimm, S. *Spectrochim. Acta* **1978**, *34A*, 395.
(34) Krimm, S.; Abe, Y. *Proc. Natl. Acad. Sci.* **1972**, *69*, 2788.
(35) Krimm, S. *Biopolymers* **1983**, *22*, 217.
(36) Cheam, T. C.; Krimm, S. *Chem. Phys. Lett.* **1984**, *107*, 613.
(37) Dybal, J.; Cheam, T. C.; Krimm, S. *J. Mol. Struct.* **1987**, *159*, 183.

Registry No. i-PMMA, 25188-98-1.